Antiviral Research 94 (2012) 288–296

Contents lists available at SciVerse ScienceDirect

Antiviral Research

journal homepage: www.elsevier.com/locate/antiviral

A hexapeptide of the receptor-binding domain of SARS corona virus spike protein blocks viral entry into host cells via the human receptor ACE2

Anna-Winona Struck [a,1], Marco Axmann [a,1], Susanne Pfefferle [b,1], Christian Drosten [b,*], Bernd Meyer [a,*]

[a] Organic Chemistry, Department of Chemistry, Faculty of Sciences, University of Hamburg, Martin Luther King Place 6, 20146 Hamburg, Germany
[b] Department of Virology, Bernhard Nocht Institute for Tropical Medicine, Bernhard-Nocht-Str. 74, 20359 Hamburg, Germany

ARTICLE INFO

Article history:
Received 14 September 2011
Revised 16 December 2011
Accepted 20 December 2011
Available online 17 January 2012

Keywords:
SARS coronavirus
Spike protein
ACE2
Entry inhibitor
Virus proliferation assay
SPR screening

ABSTRACT

In vitro infection of Vero E6 cells by SARS coronavirus (SARS-CoV) is blocked by hexapeptide Tyr-Lys-Tyr-Arg-Tyr-Leu. The peptide also inhibits proliferation of coronavirus NL63. On human cells both viruses utilize angiotensin-converting enzyme 2 (ACE2) as entry receptor. Blocking the viral entry is specific as alpha virus Sindbis shows no reduction in infectivity. Peptide ^{438}YKYRYL^{443} is part of the receptor-binding domain (RBD) of the spike protein of SARS-CoV. Peptide libraries were screened by surface plasmon resonance (SPR) to identify RBD binding epitopes. ^{438}YKYRYL^{443} carries the dominant binding epitope and binds to ACE2 with K_D = 46 μM. The binding mode was further characterized by saturation transfer difference (STD) NMR spectroscopy and molecular dynamic simulations. Based on this information the peptide can be used as lead structure to design potential entry inhibitors against SARS-CoV and related viruses.

1. Introduction

The SARS-associated corona virus (SARS-CoV) has been identified as the causative agent of severe acute respiratory syndrome (SARS) which emerged as an alerting epidemic in winter of 2002–2003 resulting in over 8000 infected cases with approximately 10% deaths (Drosten et al., 2003; Ksiazek et al., 2003; Marra et al., 2003; Peiris et al., 2003; Rota et al., 2003; WHO, 2004). SARS-CoV infects human host cells by an initial interaction of its spike glycoprotein (S) and the receptor on human cells, angiotensin-converting enzyme 2 (ACE2) (Dimitrov, 2003; Holmes, 2003; Li et al., 2003). Functional characterization of the S protein suggests that the receptor-binding domain (RBD) is located between amino acid residues 303 and 537 (Xiao et al., 2003). Flow cytometry indicated that amino acids 270–510 are the minimal receptor binding region of the S glycoprotein (Babcock et al., 2004). Further studies located the RBD from residues 318 to 510. The RBD fused to the Fc region of human IgG_1 (RBD-Fc) binds ACE2 with higher affinity ($K_D \sim 10$ nM) than does the full length S1-Ig chimera (Li et al., 2005b; Wong et al., 2004). The crystal structure of residues 306–527 of the S1 in complex with the receptor ACE2 reveals that a loop within the RBD (residues 424–494) makes all the contacts to ACE2 and is referred to as the receptor-binding motif (RBM). Six tyrosine residues are involved in direct binding to the receptor (Li et al., 2005a). Studying the virus adaptation to humans the spike protein also seems to play a major role in the species specificity of coronavirus infection. Especially, the introduction of a threonine residue at position 487 and an asparagine instead of a charged lysine residue at position 479 of the spike protein seem to be responsible for its high affinity to human ACE2 (Holmes, 2005; Li et al., 2005b; Qu et al., 2005). Yi et al. demonstrated that a single amino acid substitution (R441A) in a full-length spike protein DNA vaccine failed to induce neutralizing antibodies (NAbs) and that the same mutation yielded pseudoviruses that were unable to enter the human cells (Yi et al., 2005). Furthermore, the RBD-Fc bearing the same R441A mutation shows no affinity to ACE2 and is not capable of blocking S protein-mediated pseudovirus entry (He et al., 2006). The interaction of SARS-CoV with its receptor ACE2 is an attractive drug target as epitopes of the RBD on the spike protein may serve as leads for the design of effective entry inhibitors (Du et al., 2009). Another drug target is the fusion process of the spike protein with the host cell membrane that is characterized by the presence of two heptad repeat (HR) regions, HR1 and HR2, which are postulated to form a fusion-active conformation similar to those of other typical viral fusion proteins (Sainz et al., 2006; van der Hoek et al., 2004; Yuan et al., 2004).

* Corresponding authors. Present address: University Hospital Bonn, Institute of Virology, Sigmund-Freud-Str.25, 53127 Bonn, Germany. Tel.: +49 228 287 11055 (C. Drosten), Tel.: +49 40 42838 5913 (B. Meyer).
E-mail addresses: drosten@virology-bonn.de (C. Drosten), Bernd.Meyer@chemie.uni-hamburg.de (B. Meyer).
[1] These coauthors contributed equally to the paper.

0166-3542/$ - see front matter © 2011 Elsevier B.V. All rights reserved.
doi:10.1016/j.antiviral.2011.12.012

2. Material and methods

2.1. Peptide synthesis

Peptides were synthesized on solid phase using a Fmoc-protecting group strategy on a Fmoc-PAL-PEG-PS resin (Applied Biosystems) with *O*-(benzotriazol-1-yl)-*N*,*N*,*N*′,*N*′-tetramethyluronium tetrafluoroborate (TBTU, Iris Biotech) as activator. A MOS Ω496 synthesizer (Advanced ChemTech) and a Liberty microwave synthesizer (CEM) were used for peptide syntheses starting with 20 μmol amino groups each. After each coupling step the growing peptide was capped with an acetyl residue by 10% acetic anhydride in DMF. Cysteine residues were substituted by serines to avoid dimerization. Using trifluoroacetic acid (TFA), triisopropylsilan and H_2O (95:5:2, v/v), peptides were cleaved off the resin leaving an amide at the C-terminus. The cocktail was applied twice for 90 and 60 min, respectively. Preparative RP-HPLC was carried out on a BIOCAD 700E instrument (PerSeptive Biosystems) using a H_2O/acetonitrile gradient (0.1% TFA) on a VP250/21 Nucleodur C18 Pyramid 5 μ column (Macherey & Nagel). Peptides were characterized by MALDI-TOF mass spectrometry on a BIFLEX III instrument (Bruker Daltonics) in reflector mode using 2,5-dihydroxybenzoic acid (DHB) or α-cyano-4-hydroxycinnamic acid (CCA) as a matrix. Peptide RBD-11b (YKYRYL, Y438-L443) and related peptides were further characterized by 1D- and 2D-NMR spectroscopy (not shown).

2.2. SPR screen of peptide libraries

SPR studies were carried out using a BIACORE 3000 or Biacore T100 instrument. For all experiments a temperature of 25 °C, flow rate of 5 μL/min (BIACORE 3000) or 30 μL/min (T100), and a TBS running buffer (25 mM Tris, 0.2 M NaCl, 5 μM $ZnCl_2$ at pH 8) were used. The carboxymethylated sensorchip surface of a CM5 chip (Biacore) was activated by NHS/EDC followed by immobilization of rhACE2 (R&D Systems) in acetate-buffer (pH 3.5, Biacore). rhACE2 was obtained in TBS that had to be changed for the immobilization of the enzyme to PBS containing additional 5 μM $ZnCl_2$ (pH 7.4) using a Slide-A-Lyzer MINI Unit (Pierce Biotechnology) with a Molecular Weight Cut-off of 3500 at 4 °C for at least 12 h. Sensorgrams of RBD-11 and RBD-14 were recorded with a chip that had 54 fmol of ACE2 immobilized, that of RBD-15 on a chip with 74 fmol, those of RBD-11b and of the RBD-11b related peptide library on a chip with 100 fmol, respectively. Carboxyl groups of the activated chip surface that had not reacted with the protein were capped with ethanolamine (Biacore).

2.3. Saturation transfer difference (STD) NMR spectroscopy

2.3.1. Sample preparation

NMR samples were prepared in deuterated Tris-buffered saline (d-TBS) containing 25 mM perdeuterotris(hydroxymethyl)aminomethane (Tris-d_{11}), 0.2 M NaCl and 5 μM $ZnCl_2$ (pH 7.8) in deuterium oxide (D_2O, 99.9%). TBS of the commercial rhACE2 (R&D Systems) was changed to d-TBS in Slide-A-Lyzer MINI Units (Pierce Biotechnology) with a Molecular Weight Cut-off of 3500 twice for at least 12 h at 4 °C. YKYRYL was added from 3 mM stock solution in d-TBS with sample volume adding up to 100 μL in a 3 mm Shigemi NMR Micro Tube with c(ACE2) = 0.83 μM and peptide concentration between 14.9 and 222 μM (18–288 fold excess over ACE2).

2.3.2. Acquisition of NMR Spectra

All STD spectra were recorded at a temperature of 295 K with a spectral width of 15 ppm on a Bruker Avance DRX 700 MHz spectrometer equipped with a 5 mm inverse triple resonance cryoprobe. Selective saturation of the protein was achieved by a train of Gauss-shaped pulses of 50 ms length each, truncated at 1%, and separated by a 1 ms delay leading to a total length of saturation time of 4 s. The on-resonance irradiation of the protein was performed at a chemical shift of −0.5 ppm. Off-resonance irradiation was set at 40 ppm. Total scan number in the STD experiments was 4096. NMR spectra were multiplied by an exponential line-broadening function of 1.0 Hz prior to Fourier transformation. Water suppression was achieved by an excitation sculpting pulse sequence. Spectra processing was performed using Topspin 2.1 software (Bruker).

2.4. SARS-CoV infection assay

The SARS-CoV inhibition assay was performed as described previously (Vassilatis et al., 2003). In brief, Vero cells in 24-well plates were infected in the biosafety level 4 laboratory (BNI Hamburg) with SARS-CoV (Frankfurt isolate) at a multiplicity of infection (MOI) of 0.01. The inoculum was removed after 1 h and replaced with fresh medium complemented with different concentrations of compound. The virus RNA concentration in the supernatant was measured by real-time PCR after 2 days. RNA was prepared from 140 μL supernatant using diatomaceous silica (Pfaff et al., 1994). Quantitative real-time reverse transcription-PCR (RT-PCR) was performed with the purified RNA according to a published protocol (Drosten et al., 2003). *In vitro* transcripts of the target region were used in the PCR to generate standard curves for quantification of the virus RNA.

2.5. Molecular dynamic (MD) simulation

The MD simulations were carried out with the software Maestro/Desmond on an HP Z600 workstation (one Quadcore CPU), using the OPLS_AA/2005 force field. The starting structure was placed in a water box with orthorhombic boundary conditions and salt concentration of 200 mmol/L (SPC solvent model, 18,145 water molecules, $78 \times 88 \times 102$ Å). MD simulations over 11,000 ps were performed to equilibrate the system at 300 K. The simulation in equilibrium was performed over 3000 ps at 300 K, with the Nose-Hoover thermostat method and a relaxation time of 2.0 ps. The recording interval was 0.12 ps. Before starting MD simulations the system was minimized three times over 2000 steps, respectively. The period of the MD after equilibration with constant potential energy was used for the analysis.

Table 1
Synthetic peptide library of sixteen 12mer peptides comprising RBD-residues N318-T509 of SARS-CoV spike protein. The peptides RBD-11, RBD-14 and RBD-15 show binding to ACE2.

Peptide	Residues of the spike protein (S)	Amino acid sequence
RBD-1	N318-F329	NITNLSPFGEVF
RBD-2	N330-E341	NATKFPSVYAWE
RBD-3	R342-S353	RKKISNSVADYS
RBD-4	V354-K365	VLYNSTFFSTFK
RBD-5	S366-L377	SYGVSATKLNDL
RBD-6	S378-V389	SFSNVYADSFVV
RBD-7	K390-Q401	KGDDVRQIAPGQ
RBD-8	T402-P413	TGVIADYNYKLP
RBD-9	D414-T425	DDFMGSVLAWNT
RBD-10	R426-N437	RNIDATSTGNYN
RBD-11	Y438-R449	YKYRYLRHGKLR
RBD-12	P450-S461	PFERDISNVPFS
RBD-13	P462-N473	PDGKPSTPPALN
RBD-14	S474-T485	SYWPLNDYGFYT
RBD-15	T486-V497	TTGIGYQPYRVV
RBD-16	V498-T509	VLSFELLNAPAT

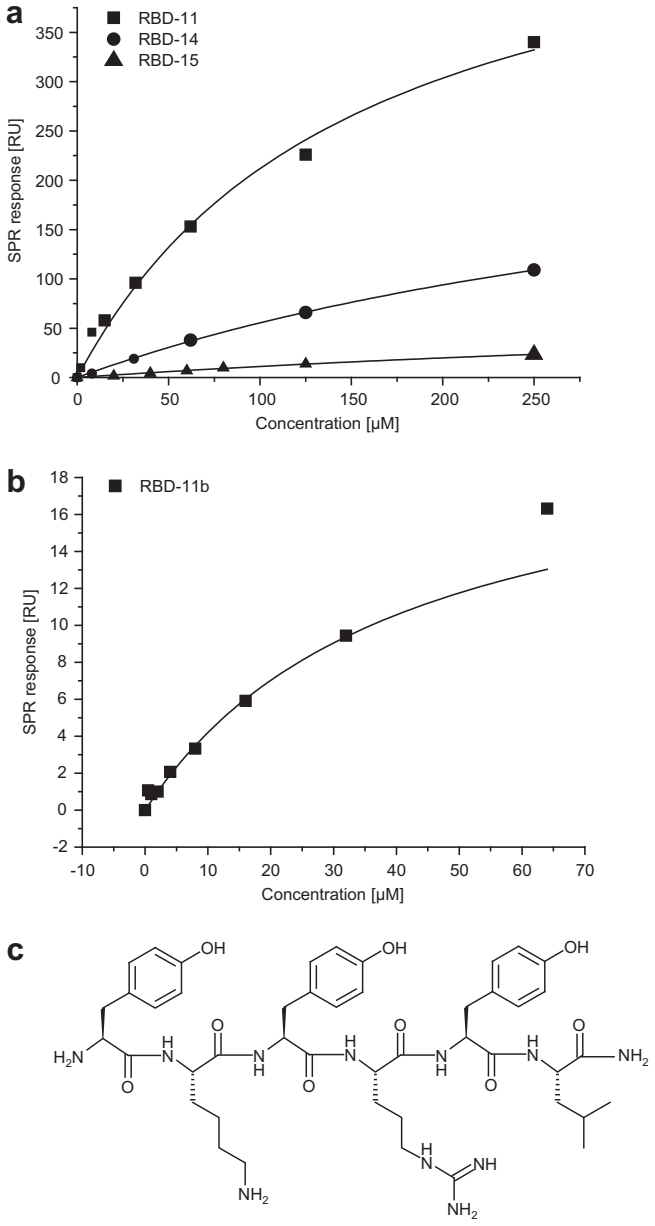

Fig. 1. SPR Screening. (A) SPR Response Units [RU] at equilibrium as a function of the concentration of RBD-11, RBD-14 and RBD-15 using immobilized ACE2 as receptor. A one site binding model was applied to fit the data and to calculate the dissociation constants. The peptides RBD-11, RBD-14 and RBD-15 bind to ACE2 with dissociation constants $K_D = 85 \pm 14$ µM for RBD-11, $K_D = 450 \pm 36$ µM for RBD-14 and $K_D = 672 \pm 168$ µM for RBD-15. It can be clearly seen that RBD-11 is the tightest binder, whereas RBD-14 and RBD-15 show only slightly lower binding constants. (B) SPR response units [RU] at equilibrium as a function of the concentration of RBD-11b (^{438}YKYRYL^{443}) using 100 fmol immobilized ACE2 as receptor. RBD-11b binds with $K_D = 46 \pm 14$ µM and shows a twofold tighter binding affinity than the corresponding dodecapeptide RBD-11. (C) Structure of the Hexapeptide RBD-11b.

3. Results and discussion

3.1. Screening of RBD peptide libraries by surface plasmon resonance (SPR)

A library of linear peptides was synthesized via solid phase synthesis using Fmoc strategy containing sixteen 12mer RBD peptides (RBD-1 to RBD-16) which together comprised residues N318-T509 (cf. Table 1). Cysteine residues were substituted by serine amino acids to avoid dimerization of the peptides. The compounds were used to identify binding motifs in interaction with the human receptor ACE2 by surface plasmon resonance (SPR) binding studies. This method allows the determination of the binding specificity, as

Table 2
Synthetic peptide library of fourteen 6mer peptides comprising RBD-residues N435-E452 and A471-S500 of SARS-CoV spike protein. The K_D of RBD-11b (YKYRYL) is 46 µM. The on- and off-rates are 3.7×10^3 M^{-1} s^{-1} and 0.17 s^{-1}, respectively. Peptide RBD-11c (RYLRHG) shows $K_D = 770$ µM, $k_{on} = 3.1 \times 10^2$ M^{-1} s^{-1} and $k_{off} = 0.24$ s^{-1}.

Peptide	Residues of the spike protein (S)	Amino acid sequence
RBD-11a	N435-Y440	NYNYKY
RBD-11b	Y438-L443	YKYRYL
RBD-11c	R441-G446	RYLRHG
RBD-11d	R444-R449	RHGKLR
RBD-11e	K447-E452	KLRPFE
RBD-14a	A471-W476	ALNSYW
RBD-14b	S474-N479	SYWPLN
RBD-14c	P477-G482	PLNDYG
RBD-14d	D480-T485	DYGFYT
RBD-15a	F483-G488	FYTTTG
RBD-15b	T486-Y491	TTGIGY
RBD-15c	I489-Y494	IGYQPY
RBD-15d	Q492-V497	QPYRVV
RBD-15e	R495-S500	RVVVLS

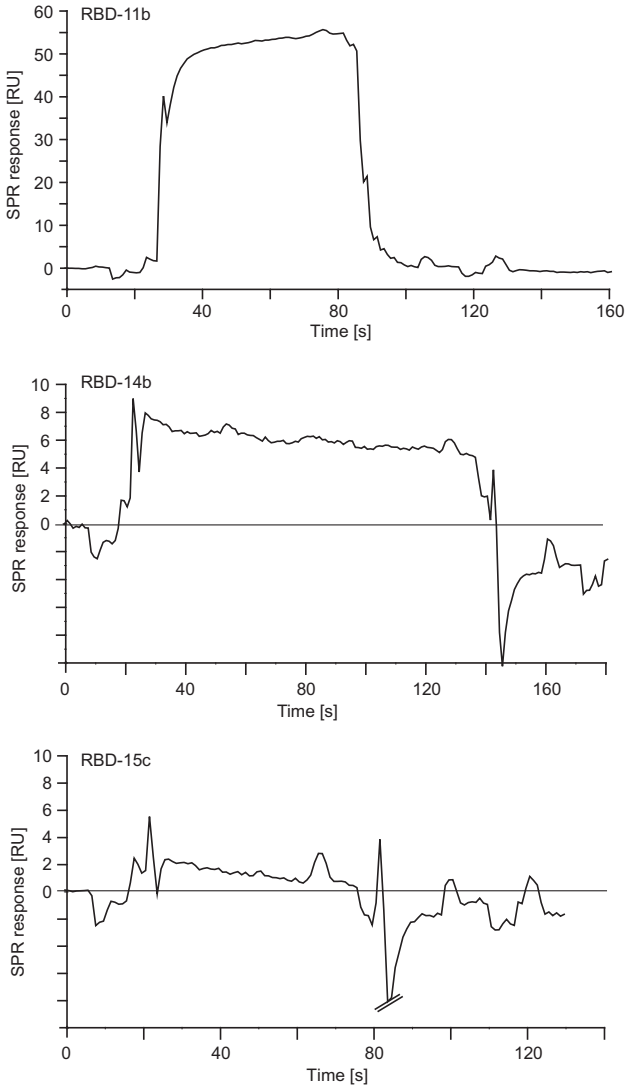

Fig. 2. SPR sensorgram data for the screening of selected RBD peptides. SPR sensorgrams using immobilized ACE2 as receptor. It can be clearly seen that RBD-11b shows the highest SPR response signal, whereas RBD-14b shows only weak interaction to ACE2. For RBD-15c is no interaction observable.

well as the association and dissociation rates of ligands interacting with protein receptors. The receptor protein ACE2 was immobilized on the sensor chip and the peptides were passed over the sensor surface. The affinity of the interaction is determined from the level of binding at equilibrium as a function of sample concentration and can also be determined from analysis of the binding kinetics. SPR screening of the sixteen 12mer RBD peptides resulted in positive responses of three peptides, i.e. RBD-11 (Y438-R449 – YKYRYLRHGKLR), RBD-14 (S474-T485 – SYWPLNDYGFYT) and RBD-15 (T486-V497 – TTGIGYQPYRVV), respectively. All other RBD peptides showed no or insignificantly small response signals and were thus not interacting with ACE2. To analyze whether the interaction of the peptides RBD-11, RBD-14 and RBD-15 is based on a specific binding event, the SPR sensorgrams of each compound were recorded at several different concentrations. The signal at equilibrium measured in response units [RU] obtained from the sensorgrams was plotted against the concentration of ligand passed over the sensor surface (cf. Fig 1). Assuming a one site binding model the specific saturable binding affinity of the ligand peptides is calculated to K_D = 85 ± 14 μM for RBD-11, K_D = 450 ± 36 μM for RBD-14 and K_D = 672 ± 168 μM for RBD-15. The SPR sensorgrams were also used to determine kinetic parameters of binding, the association rate constant k_{on} [$s^{-1}M^{-1}$] and the dissociation rate constant k_{off} [s^{-1}]. RBD-11 shows a fivefold higher association rate constant $k_{on} = 1.8 \times 10^3\ s^{-1}M^{-1}$ compared to RBD-14 and RBD-15 with $k_{on} = 3.7 \times 10^2\ s^{-1}M^{-1}$ and $3.2 \times 10^2\ s^{-1}M^{-1}$, respectively. The dissociation rate of all three peptides is comparable with $k_{off} = 0.12\ s^{-1}$ (RBD-11), $0.16\ s^{-1}$ (RBD-14) and $0.15\ s^{-1}$ (RBD-15), respectively. The dissociation constant $K_D = k_{off}/k_{on}$ resulting from analysis of the kinetic data of the peptides are K_D = 67 μM (RBD-11), 430 μM (RBD-14) and 450 μM (RBD-15) in excellent agreement with the dissociation constants obtained from thermodynamic data analysis. The on-rates suggest that the bioactive conformation of peptide RBD-11 is more similar to its solution conformation than for RBD-14 and RBD-15.

Peptides RBD-11, RBD-14 and RBD-15 contain 60% of the residues, namely Y440, Y442, Y475, N479, Y484, T486, T487, G488 and Y491 that were identified by X-ray crystal structure analysis to be in contact with ACE2 (Li et al., 2005a). Several mutations in the viral protein were necessary to change the host organisms from wild animals, like civet cats, to humans, i.e. S487T and K479N (Holmes, 2005; Li et al., 2005b; Qu et al., 2005). These amino acids are included in the peptides RBD-14 and RBD-15. In a screening of a library Hu et al. identified a 33mer peptide (A471-L503) that

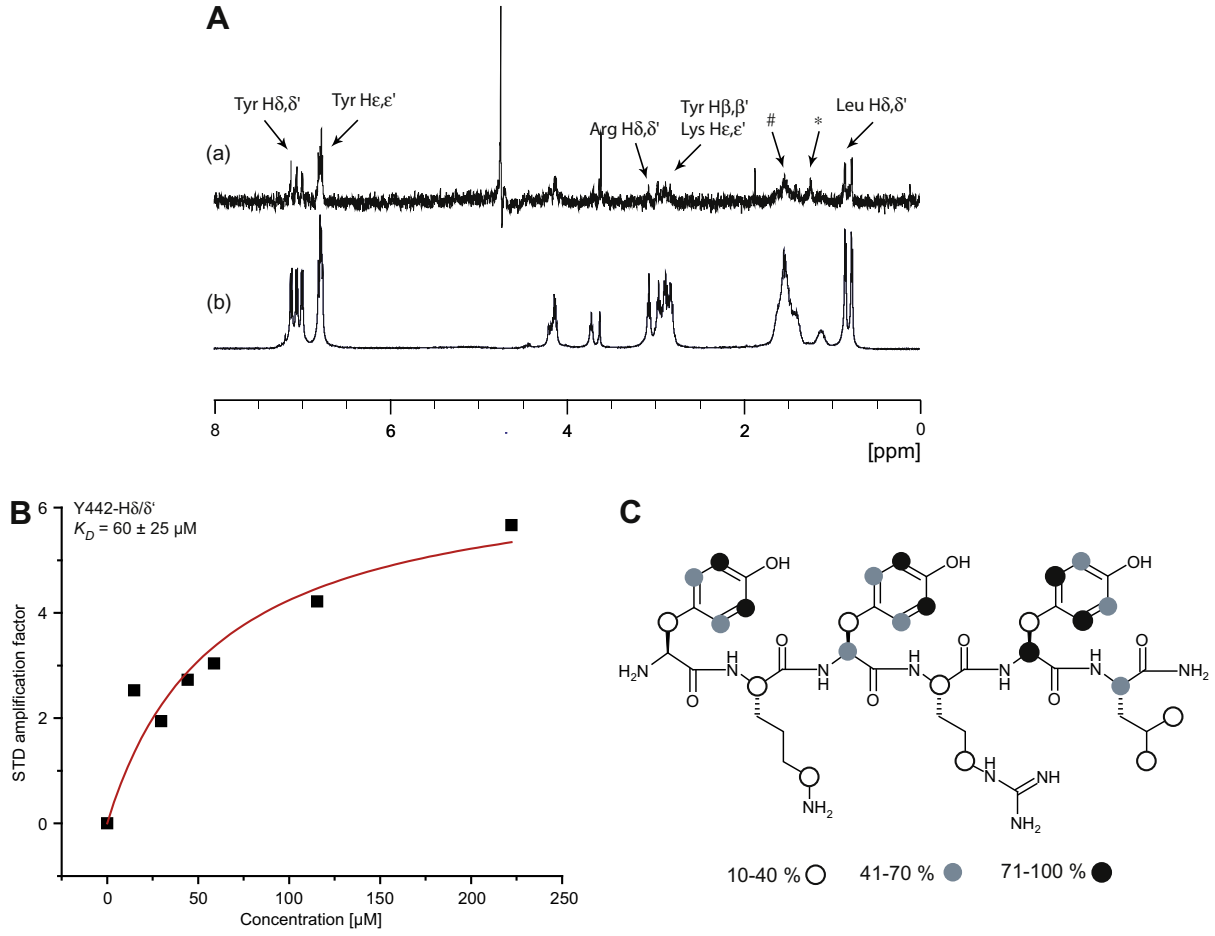

Fig. 3. STD NMR spectroscopy of RBD-11b and ACE2. (A) Saturation transfer difference NMR spectra of RBD-11b binding to ACE2. (a) ^{1}H STD NMR spectrum of an ACE2 solution (c = 0.83 μM) together with RBD-11b (c = 59 μM, 72 fold excess over ACE2) at 700 MHz (4 K scans) in d-TBS shows significant STD effects for the aromatic tyrosine residues between 6.7 and 7.1 ppm. Protons Hδ,δ of R441 (3.00 ppm) and L443 (0.72, 0.80 ppm) clearly receive saturation due to their proximity to the receptor molecule. STD NMR signals between 2.7 and 2.9 ppm show saturation of β-protons of all three tyrosine residues and of Lys Hε,ε. (b) Normal ^{1}H NMR spectrum of a 3.0 mM solution of the hexapeptide RBD-11b at 700 MHz. In all spectra water was suppressed by an excitation sculpting pulse sequence and spectra were acquired in d-TBS at 295 K in a 100 μL (Hwang and Shaka, 1995). (B) Determination of binding affinity from STD NMR titration data. The titration curve of the aromatic protons Hδ,δ of Tyr442 is shown. The K_D value was determined from the STD NMR titration by using the one site binding model. The resulting K_D value is 60 ± 25 μM. (C) STD NMR epitope mapping of RBD-11b. The spots indicate the range of relative STD% for the protons that were saturated according to their proximity to the human receptor protein ACE2. A strong binding is detected for the aromatic protons of the three tyrosines. The highest degree of saturation of 4.1 STD% (absolute) obtained for Hε,ε of Tyr440 was set to 100% relative STD.

could inhibit the binding of RBD to ACE2 and the plaque formation of SARS-CoV in Vero cells with an EC_{50} value of 41.6 μM (Hu et al., 2005). Ho et al. showed biological activities of small peptides derived from S protein to inhibit the spike protein and ACE2 interaction. Among others peptide SP-8 (residues 483–494, FYTTTGIGYQPY), which overlaps in sequence with the identified peptides RBD-14 and RBD-15, shows inhibitory activity at a 1 million fold excess relative to ACE2 (Ho et al., 2006). However, the 20mer peptide P4 comprising residues 470–489 (PALNCYWPLNDYGFYTTSGI) of Zheng et al. overlapping with peptide RBD-14 shows no inhibition in a cytopathic effect (CPE)-based assay (Zheng et al., 2005). In contrast, as mentioned above, the partially overlapping peptides A471-L503 (Hu et al., 2005) and SP-8 (Ho et al., 2006) showed virus inhibition in their respective assays.

To further characterize the binding epitope we synthesized a second peptide library of fourteen hexamer peptides comprising residues N435-E452 (RBD-11a to RBD-11e) and A471-S500 (RBD-14a to RBD-14d and RBD-15a to RBD-15e) with an overlap of three amino acids in each sequence (cf. Table 2).

These peptides were used to further locate strongly interacting amino acids by SPR and saturation transfer difference (STD) NMR spectroscopy. SPR screening was performed with ligand concentrations of up to 500 μM in TBS and 48 fmol of immobilized ACE2. RBD-11b (Y438-L443; YKYRYL) showed the highest SPR response signal of 51 RU at a concentration of 250 μM. Also the flanking peptides RBD-11a (N435-Y440; NYNYKY) and RBD-11c (R441-G446; RYLRHG) showed significant binding of 5 RU (c = 250 μM) and 34 RU (c = 500 μM), respectively. The SPR response of peptides RBD-14a (A471-W476; ALNSYW) and RBD-14b (S474-N479; SYWPLN) was comparable to that of RBD-11a (5 and 7 RU, respectively) (cf. Fig. 2). The other hexapeptides gave no significant SPR signal. Therefore, only peptide RBD-11b (Y438-L443; YKYRYL) was further investigated by SPR and STD NMR experiments. A concentration dependent SPR affinity plot was performed with 110 fmol of receptor protein immobilized. Fig. 1 shows the concentration dependent binding of RBD-11b (YKYRYL) by SPR resulting in a dissociation constant $K_D = 46 \pm 14$ μM which is two-fold higher affinity than that of peptide RBD-11. The binding kinetics are $k_{on} = 3.7 \times 10^3\ s^{-1}M^{-1}$ and $k_{off} = 0.17\ s^{-1}$ and also result in a dissociation constant of $K_D = 46$ μM. The two-fold increase of the binding affinity compared to RBD-11 results from a two-fold higher on-rate which is probably due to a better defined conformation in solution such that binding can occur more rapidly. The off-rate is the same as found for the dodecapeptide RBD-11.

3.2. Affinity determination and epitope mapping by saturation transfer difference (STD) NMR spectroscopy

STD NMR spectroscopy is a well-established method to characterize ligand–protein interactions (Mayer and Meyer, 1999, 2001). Here it was used to determine dissociation constant and binding epitope of the interaction of RBD-11b with a soluble construct of the receptor protein ACE2 in deuterated TRIS-buffered D_2O. Fig. 3 shows the ^1H STD NMR spectrum of RBD-11b (YKYRYL) and receptor ACE2 at a 72 fold excess of the ligand over the protein. Dependence of the STD amplification factor on the concentration of RBD-11b yields the K_D value. A one site binding model fits the experimental data well and gives K_D values in the low micromolar range: Hδ,δ′ of the Tyr442 results in $K_D = 60 \pm 25$ μM. The binding epitope was determined from STD spectra at a 144 fold excess of the ligand. It shows that all tyrosine residues have a close contact to ACE2. Furthermore, the Hα atom of Arg441 also has a close proximity to the receptor surface. The Hα atoms of Tyr440 and Leu443 interact also strongly with the cellular receptor. The positively charged groups of lysine and arginine side chains also show

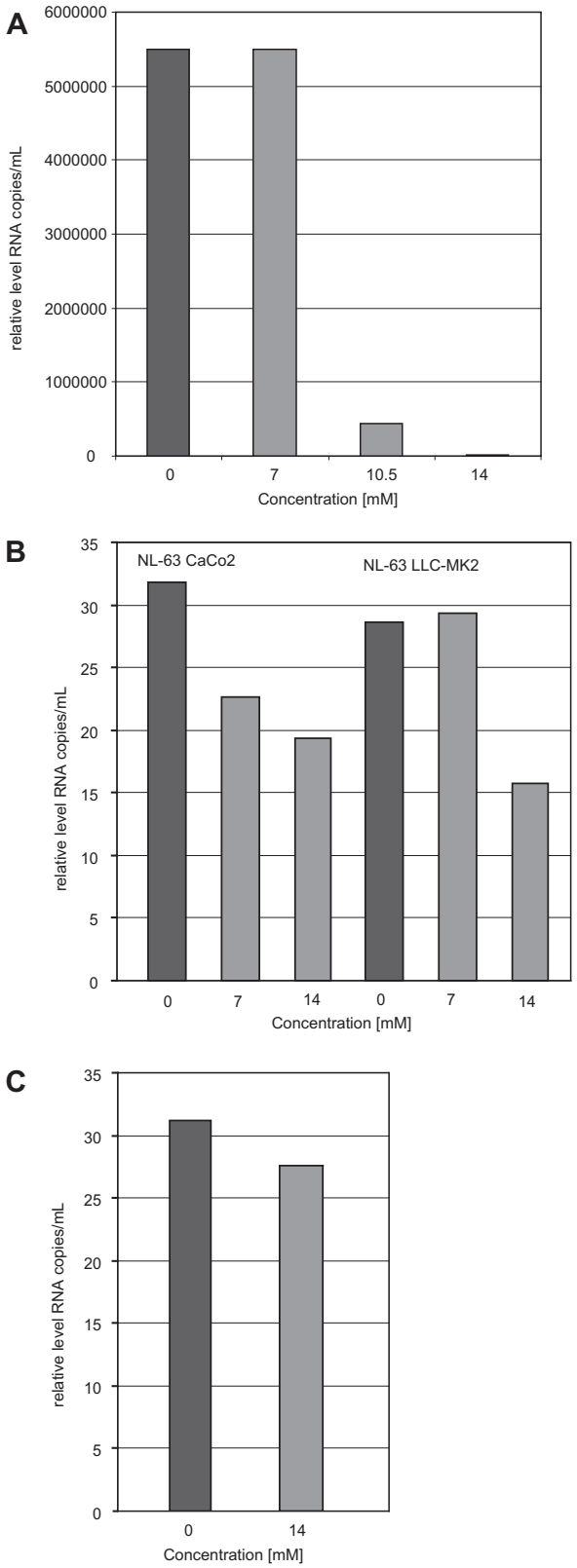

Fig. 4. Inhibition of virus replication in cells by different concentrations of RBD-11b. (A) Inhibition of SARS corona virus replication in VeroE6 cells. The bar plot indicates the relative level of RNA copies per mL as a function of the RBD-11b concentration (quantified by real-time PCR). The peptide shows a concentration dependent decrease of virus RNA. (B) Inhibition of NL63 virus in two cell lines. The results for $CaCo_2$ cells are shown on the left side and the results for LLC-MK2 cells are shown on the right side of the figure. (C) Inhibition of alpha virus Sindbis replication in VeroE6 cells. No significant inhibitory effect is observed.

moderately strong interactions with the surface. The C-terminal leucine seems to be involved in a hydrophobic contact via its side chain. The highest level of saturation of 4.1% STD (absolute) is found for the Hε,ε of Tyr440. The X-ray crystal structure analysis of the complex of RBD (residues 318–510) with ACE2 shows only contacts of Tyr440 and Tyr442 of the RBD with ACE2 (Li et al., 2005a). However, in the isolated hexapeptide YKYRYL, Tyr438 is also binding to ACE2. According to mutation studies Arg441 of SARS-CoV spike protein is important for binding affinity (He et al., 2006). This fact is confirmed by STD NMR analysis. The side chain protons Hδ,δ of Arg441 exhibit 0.7% absolute STD, which suggests an ionic interaction of the guanidinium group with the receptor molecule. The X-ray structure of the complex revealed no direct contact between Arg441 of RBD and ACE2. Thus in the free form the hexapeptide adopts a different binding mode and conformation compared to the case when integrated into the RBD. Lys439 also makes a contact via its positively charged group evidenced by the STD effect on the Hε,ε protons that receive a saturation of 0.6%. Protons of Leu443 methyl groups show a STD effect of 0.6% and 0.9% STD, respectively, indicating a contact of the methyl groups to the receptor.

3.3. Inhibition of SARS-CoV replication in cell culture

The biological activity of the lead structure RBD-11b (Y438-L443; YKYRYL) was assayed with respect to its ability to inhibit virus replication in cell culture (Drosten et al., 2004). VeroE6 cells were infected with the SARS-CoV isolate Frankfurt. As described previously, growth of the virus in Vero cells is not associated with a cytopathic effect (Vassilatis et al., 2003). Cells were infected with a virus titer of 0.01 MOI. The inoculum was removed after 1 h and replaced with fresh medium complemented with different concentrations of peptide RBD-11b in a one-time dose. Two days post infection virus RNA concentration in the supernatant was measured by real-time PCR (cf. Fig. 4). There was no evidence for toxicity of the compound in the concentration range tested with MTT cell proliferation assay on subconfluent cells. After two days a one-time dose of the peptide RBD-11b (YKYRYL, 10.5 mM) reduced the virus RNA level compared to the untreated control by a factor of 10. Further, the inhibition of virus proliferation by the peptide is concentration dependent. After two days, relative to an untreated control virus RNA is reduced by a factor of 600 at a 14 mM concentration of the peptide. The final amount of virus RNA is in fact lower than the initially added amount. These data suggest that the hexapeptide blocks indeed the binding site necessary for the initial viral attachment to the human receptor ACE2 and effectively inhibits viral entry into Vero cells. Thus, the virus is not capable to replicate and viral particles are exposed to the degradation process. These results are in good agreement with the occupation of the receptor's binding site given the peptide's dissociation constant of K_D = 46 μM. At peptide concentrations of 7 mM the occupation of binding sites is 99.3%, at 10.5 mM it is 99.6% and at 14 mM 99.7%, respectively.

The peptide inhibits the infection of the corona virus specifically. This is proven by the fact that RBD-11b does not inhibit infection of Vero cells with the alpha virus Sindbis, which cause high fever in humans.(Tesh, 1982) Furthermore, the peptide was also tested in an inhibition assay with another corona virus NL63 in LLC-MK2 and CaCo2 cells. NL63 corona virus causes severe colds in human and uses ACE2 also as a functional receptor.(van der Hoek et al., 2004; Wu et al., 2009) Inhibitory effects were observed for both cell lines at a concentration of 14 mM. For CaCo2 cells inhibition is also observed at a peptide concentration of 7 mM.

3.4. Synthesis of RBD-11b related peptides with point mutations

We have synthesized various hexapeptides closely related to peptide RBD-11b (YKYRYL) including an alanine scan library and analyzed by SPR the importance of individual amino acids for binding to ACE2. The alanine scan reveals that the tripeptide motif ^{439}KYR^{441} is essential for the binding (cf. Fig. 5). The other binding curves show that the positively charged side chains of the amino acids Lys439 and Arg441 may be important for the receptor binding. No binding was observed for the peptides YDYRYL and YKYDYL with the negatively charged aspartate replacing the positively charged Lys and Arg. Changing positively charged residues to uncharged residues (K439S, R441S) reduces the binding affinity but does not abolish it. These results indicate a clear role of Lys439 and Arg441 in the binding process in agreement with the STD NMR data shown above.

3.5. Molecular dynamic (MD) simulation of ACE2 and the peptide RBD-11b (YKYRYL)

The binding mode of peptide RBD-11b to the human receptor ACE2 was also analyzed by docking of the peptide to the binding site followed by a molecular dynamics (MD) simulation that was recorded for 3000 ps in equilibrium using the OPLS_AA/2005 force field as realized in the program Desmond (Schrödinger) (Jorgensen

A

Peptide	Amino acid sequence
1	^{438}Y K Y R Y L^{443}
2	**A** K Y R Y L
3	Y **A** Y R Y L
4	Y K **A** R Y L
5	Y K Y **A** Y L
6	Y K Y R **A** L
7	Y K Y R Y **A**

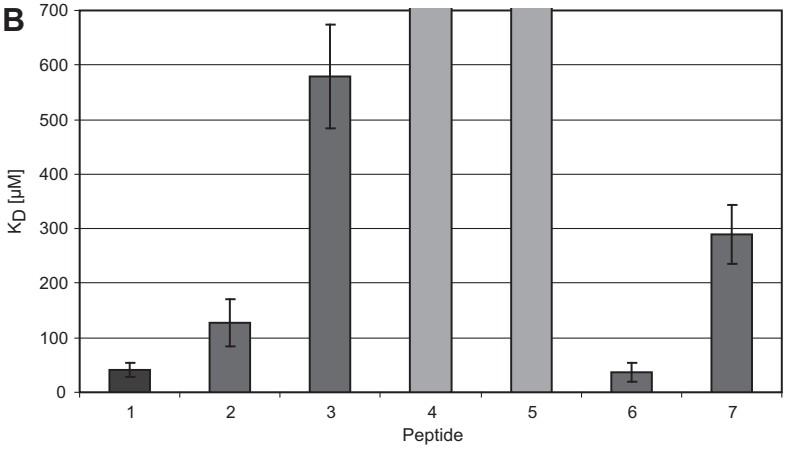

Fig. 5. Synthetic alanine scan of the lead compound RBD-11b. (A) Sequence of alanine scan peptides. (B) The dissociation constants K_D of the alanine scan. The K_D values are obtained from thermodynamic data analysis of SPR studies. K_D of the lead compound RBD-11b is show in dark gray, peptides with specific interaction in gray and peptides with no interaction to ACE2 are shown in light gray.

et al., 1996). The conformation of peptide RBD-11b in the crystal structure of the RBD of the viral spike protein in complex with the receptor ACE2 was used as starting structure (Li et al., 2005a). The protein peptide complex was placed in a water box with 18,145 water molecules and a sodium chloride concentration of 0.2 mol/L. The peptide shows high dynamics during the MD but stays always in contact with the receptor surface. Fig. 6 shows the starting and the final conformation of the complex. The side chains of amino acids Tyr440 and Tyr442 interact with ACE2 in the crystal structure. At the end of the MD simulation Lys439, Tyr440 and Arg441 show interactions with the receptor. The binding mode of hexapeptide RBD-11b to ACE2 differs from the binding mode of the hexapeptide as part of the full length S protein. The positively charged residue of Lys439 forms ionic interactions with the carboxyl group of Glu23 of ACE2. The average distance from the Lysine ε-nitrogen atom and an oxygen atom of the carboxyl group over the course of the MD simulation is 3.08 ± 0.74 Å. The guanidinium group (Nη) of Arg441 interacts with the carboxyl group of Asp30 of the receptor with an average distance of 3.42 ± 0.91 Å. The crystal structure shows the first three carbohydrate units of a high mannose *N*-glycan on the receptor surface resolved. In the MD simulation Tyr440 shows contact to the glycan molecule by interaction of its aromatic residue with the second *N*-acetylglucosamine and the mannose residue. The average distance of the interaction of the aromatic ring with the *N*-acetylglucosamine is 5.11 ± 0.88 Å and with the mannose 5.97 ± 0.77 Å, respectively.

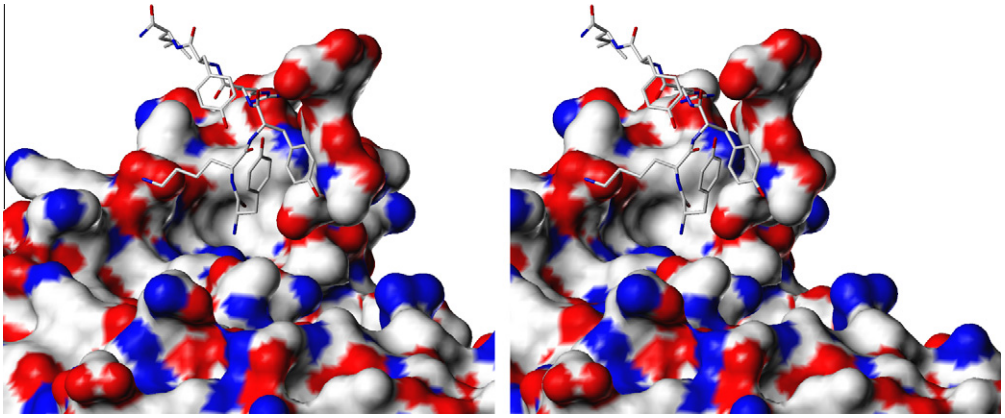

Fig. 6. Molecular modeling studies of ACE2 and RBD-11b. Stereo view of the conformation of the peptide RBD-11b in the peptide receptor complex after 3 ns molecular dynamic simulation. The peptide conformation and the receptor surface are shown in atom color.

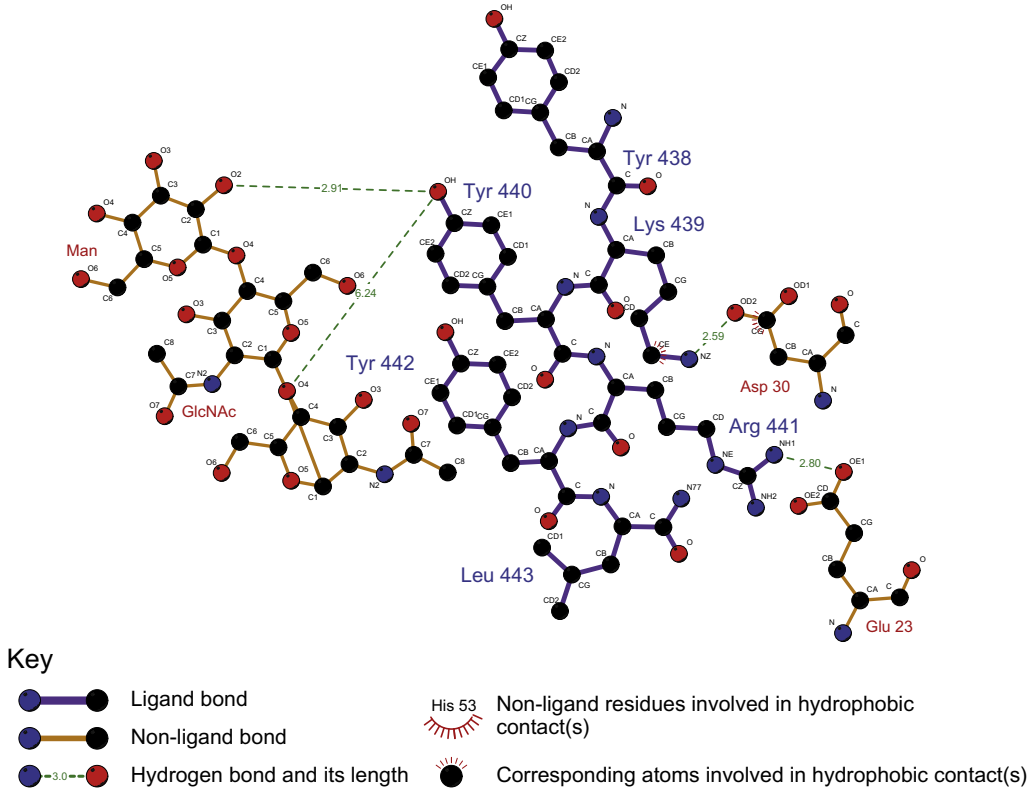

Fig. 7. Schematic representation of the interaction between ACE2 and RBD-11b. The figure was calculated with the LIGPLOT program for the end frame of the MD simulation (Wallace et al., 1995).

During the MD simulations the peptide shifted 5.4 Å at the C-terminus and 17.2 Å at the N-terminus from its initial position to its final pose (Fig. 7). The results of the MD studies support the affinity data obtained from the alanine scan, which indicates that the tripeptide motif ^{439}KYR^{441} is important for the binding to ACE2.

4. Conclusion

SARS belongs to the major new emerging virus diseases. In 2003 it caused a major outbreak with about 1000 deaths. It is a respiratory disease with about 10% mortality that is caused by a variant of the common coronaviruses (SARS-CoV). Rigid political measures helped to contain the epidemic within a short period of time. So far no specific treatment against SARS is available. In search for molecules that can specifically block the attachment of the virus to the human cell, we analyzed binding modes of viral peptides to the human receptor. We identified and characterized the focal point of the viral protein that is used by the virus for its attachment to the human cell. We found a hexapeptide in the receptor-binding domain (RBD) of the S protein of SARS-CoV that carries a significant portion of the binding affinity of the virus to the human cell. The S protein mediates the attachment of the virus to its functional receptor ACE2. The attachment of the virus to ACE2 does not interfere with the natural function of the receptor. Therefore, it is easy to block the attachment site of the virus in the upper respiratory tract as a preventive measure against SARS. We could clearly demonstrate that hexapeptide Tyr–Lys–Tyr–Arg–Tyr–Leu reduces viral infection of epithelial cells, as found in the upper respiratory tract, by a factor of 600. This peptide was shown to be specific against coronaviruses that attach to the ACE2 receptor. Its mode of action is specific as it does not interfere with other infections by viruses that utilize different receptors, like alpha virus Sindbis. Combination of several biophysical methods, e.g. SPR, STD NMR and molecular dynamics simulations, were used to characterize the specific binding mode of the inhibitory peptide. Although there is currently no SARS outbreak the need of an antiviral drug, e.g. based on the hexapeptide, is still present. A viral reservoir is present in wild animals like bats and civet cats and a new epidemic is likely someday.

References

Babcock, G.J., Esshaki, D.J., Thomas, W.D.J., Ambrosino, D.M., 2004. Amino acids 270–510 of the severe acute respiratory syndrome coronavirus spike protein are required for interaction with receptor. J. Virol. 78, 4552–4560.

Dimitrov, D.S., 2003. The secret life of ACE2 as a receptor for the SARS virus. Cell 115, 652–653.

Drosten, C., Chiu, L.L., Panning, M., Leong, H.N., Preiser, W., Tam, J.S., Gunther, S., Kramme, S., Emmerich, P., Ng, W.L., Schmitz, H., Koay, E.S., 2004. Evaluation of advanced reverse transcription-PCR assays and an alternative PCR target region for detection of severe acute respiratory syndrome-associated coronavirus. J. Clin. Microbiol. 42, 2043–2047.

Drosten, C., Gunther, S., Preiser, W., van der Werf, S., Brodt, H.R., Becker, S., Rabenau, H., Panning, M., Kolesnikova, L., Fouchier, R.A., Berger, A., Burguiere, A.M., Cinatl, J., Eickmann, M., Escriou, N., Grywna, K., Kramme, S., Manuguerra, J.C., Muller, S., Rickerts, V., Sturmer, M., Vieth, S., Klenk, H.D., Osterhaus, A.D., Schmitz, H., Doerr, H.W., 2003. Identification of a novel coronavirus in patients with severe acute respiratory syndrome. N. Engl. J. Med. 348, 1967–1976.

Du, L., He, Y., Zhou, Y., Liu, S., Zheng, B.J., Jiang, S., 2009. The spike protein of SARS-CoV – a target for vaccine and therapeutic development. Nat. Rev. Microbiol. 7, 226–236.

He, Y., Li, J., Jiang, S., 2006. A single amino acid substitution (R441A) in the receptor-binding domain of SARS coronavirus spike protein disrupts the antigenic structure and binding activity. Biochem. Biophys. Res. Commun. 344, 106–113.

Ho, T.Y., Wu, S.L., Chen, J.C., Wei, Y.C., Cheng, S.E., Chang, Y.H., Liu, H.J., Hsiang, C.Y., 2006. Design and biological activities of novel inhibitory peptides for SARS-CoV spike protein and angiotensin-converting enzyme 2 interaction. Antiviral Res. 69, 70–76.

Holmes, K.V., 2003. SARS-associated coronavirus. N. Engl. J. Med. 348, 1948–1951.

Holmes, K.V., 2005. Structural biology: adaptation of SARS coronavirus to humans. Science 309, 1822–1823.

Hu, H., Li, L., Kao, R.Y., Kou, B., Wang, Z., Zhang, L., Zhang, H., Hao, Z., Tsui, W.H., Ni, A., Cui, L., Fan, B., Guo, F., Rao, S., Jiang, C., Li, Q., Sun, M., He, W., Liu, G., 2005. Screening and identification of linear B-cell epitopes and entry-blocking peptide of severe acute respiratory syndrome (SARS)-associated coronavirus using synthetic overlapping peptide library. J. Comb. Chem. 7, 648–656.

Hwang, T.L., Shaka, A.J., 1995. Water suppression that works – excitation sculpting using arbitrary wave-forms and pulsed-field gradients. J. Magn. Reson., Ser. A 112, 275–279.

Jorgensen, W.L., Maxwell, D.S., Tirado-Rives, J., 1996. Development and testing of the OPLS all-atom force field on conformational energetics and properties of organic liquids. J. Am. Chem. Soc. 118, 11225–11236.

Ksiazek, T.G., Erdman, D., Goldsmith, C.S., Zaki, S.R., Peret, T., Emery, S., Tong, S., Urbani, C., Comer, J.A., Lim, W., Rollin, P.E., Dowell, S.F., Ling, A.E., Humphrey, C.D., Shieh, W.J., Guarner, J., Paddock, C.D., Rota, P., Fields, B., DeRisi, J., Yang, J.Y., Cox, N., Hughes, J.M., LeDuc, J.W., Bellini, W.J., Anderson, L.J., 2003. A novel coronavirus associated with severe acute respiratory syndrome. N. Engl. J. Med. 348, 1953–1966.

Li, F., Li, W., Farzan, M., Harrison, S.C., 2005a. Structure of SARS coronavirus spike receptor-binding domain complexed with receptor. Science 309, 1864–1868.

Li, W., Moore, M.J., Vasilieva, N., Sui, J., Wong, S.K., Berne, M.A., Somasundaran, M., Sullivan, J.L., Luzuriaga, K., Greenough, T.C., Choe, H., Farzan, M., 2003. Angiotensin-converting enzyme 2 is a functional receptor for the SARS coronavirus. Nature 426, 450–454.

Li, W., Zhang, C., Sui, J., Kuhn, J.H., Moore, M.J., Luo, S., Wong, S.K., Huang, I.C., Xu, K., Vasilieva, N., Murakami, A., He, Y., Marasco, W.A., Guan, Y., Choe, H., Farzan, M., 2005b. Receptor and viral determinants of SARS-coronavirus adaptation to human ACE2. EMBO J. 24, 1634–1643.

Marra, M.A., Jones, S.J., Astell, C.R., Holt, R.A., Brooks-Wilson, A., Butterfield, Y.S., Khattra, J., Asano, J.K., Barber, S.A., Chan, S.Y., Cloutier, A., Coughlin, S.M., Freeman, D., Girn, N., Griffith, O.L., Leach, S.R., Mayo, M., McDonald, H., Montgomery, S.B., Pandoh, P.K., Petrescu, A.S., Robertson, A.G., Schein, J.E., Siddiqui, A., Smailus, D.E., Stott, J.M., Yang, G.S., Plummer, F., Andonov, A., Artsob, H., Bastien, N., Bernard, K., Booth, T.F., Bowness, D., Czub, M., Drebot, M., Fernando, L., Flick, R., Garbutt, M., Gray, M., Grolla, A., Jones, S., Feldmann, H., Meyers, A., Kabani, A., Li, Y., Normand, S., Stroher, U., Tipples, G.A., Tyler, S., Vogrig, R., Ward, D., Watson, B., Brunham, R.C., Krajden, M., Petric, M., Skowronski, D.M., Upton, C., Roper, R.L., 2003. The Genome sequence of the SARS-associated coronavirus. Science 300, 1399–1404.

Mayer, M., Meyer, B., 1999. Characterization of ligand binding by saturation transfer difference NMR spectroscopy. Angew. Chem. Int. Edit. 38, 1784–1788.

Mayer, M., Meyer, B., 2001. Group epitope mapping by saturation transfer difference NMR to identify segments of a ligand in direct contact with a protein receptor. J. Am. Chem. Soc. 123, 6108–6117.

Peiris, J.S., Lai, S.T., Poon, L.L., Guan, Y., Yam, L.Y., Lim, W., Nicholls, J., Yee, W.K., Yan, W.W., Cheung, M.T., Cheng, V.C., Chan, K.H., Tsang, D.N., Yung, R.W., Ng, T.K., Yuen, K.Y., 2003. Coronavirus as a possible cause of severe acute respiratory syndrome. Lancet 361, 1319–1325.

Pfaff, M., Tangemann, K., Muller, B., Gurrath, M., Muller, G., Kessler, H., Timpl, R., Engel, J., 1994. Selective recognition of cyclic RGD peptides of NMR defined conformation by alpha IIb beta 3, alpha V beta 3, and alpha 5 beta 1 integrins. J. Biol. Chem. 269, 20233–20238.

Qu, X.X., Hao, P., Song, X.J., Jiang, S.M., Liu, Y.X., Wang, P.G., Rao, X., Song, H.D., Wang, S.Y., Zuo, Y., Zheng, A.H., Luo, M., Wang, H.L., Deng, F., Wang, H.Z., Hu, Z.H., Ding, M.X., Zhao, G.P., Deng, H.K., 2005. Identification of two critical amino acid residues of the severe acute respiratory syndrome coronavirus spike protein for its variation in zoonotic tropism transition via a double substitution strategy. J. Biol. Chem. 280, 29588–29595.

Rota, P.A., Oberste, M.S., Monroe, S.S., Nix, W.A., Campagnoli, R., Icenogle, J.P., Penaranda, S., Bankamp, B., Maher, K., Chen, M.H., Tong, S., Tamin, A., Lowe, L., Frace, M., DeRisi, J.L., Chen, Q., Wang, D., Erdman, D.D., Peret, T.C., Burns, C., Ksiazek, T.G., Rollin, P.E., Sanchez, A., Liffick, S., Holloway, B., Limor, J., McCaustland, K., Olsen-Rasmussen, M., Fouchier, R., Gunther, S., Osterhaus, A.D., Drosten, C., Pallansch, M.A., Anderson, L.J., Bellini, W.J., 2003. Characterization of a novel coronavirus associated with severe acute respiratory syndrome. Science 300, 1394–1399.

Sainz, B.J., Mossel, E.C., Gallaher, W.R., Wimley, W.C., Peters, C.J., Wilson, R.B., Garry, R.F., 2006. Inhibition of severe acute respiratory syndrome-associated coronavirus (SARS-CoV) infectivity by peptides analogous to the viral spike protein. Virus Res. 120, 146–155.

Tesh, R.B., 1982. Arthritides caused by mosquito-borne viruses. Annu. Rev. Med. 33, 31–40.

van der Hoek, L., Pyrc, K., Jebbink, M.F., Vermeulen-Oost, W., Berkhout, R.J., Wolthers, K.C., Wertheim-van Dillen, P.M., Kaandorp, J., Spaargaren, J., Berkhout, B., 2004. Identification of a new human coronavirus. Nat. Med. 10, 368–373.

Vassilatis, D.K., Hohmann, J.G., Zeng, H., Li, F., Ranchalis, J.E., Mortrud, M.T., Brown, A., Rodriguez, S.S., Weller, J.R., Wright, A.C., Bergmann, J.E., Gaitanaris, G.A., 2003. The G protein-coupled receptor repertoires of human and mouse. Proc. Natl. Acad. Sci. USA 100, 4903–4908.

Wallace, A.C., Laskowski, R.A., Thornton, J.M., 1995. LIGPLOT: a program to generate schematic diagrams of protein-ligand interactions. Protein Eng. 8, 127–134.

WHO, 2004. SARS-lessons from a new disease, World Health Report 2003, World Health Organisation.

Wong, S.K., Li, W., Moore, M.J., Choe, H., Farzan, M., 2004. A 193-amino acid fragment of the SARS coronavirus S protein efficiently binds angiotensin-converting enzyme 2. J. Biol. Chem. 279, 3197–3201.

Wu, K., Li, W., Peng, G., Li, F., 2009. Crystal structure of NL63 respiratory coronavirus receptor-binding domain complexed with its human receptor. Proc. Natl. Acad. Sci. USA 106, 19970–19974.

Xiao, X., Chakraborti, S., Dimitrov, A.S., Gramatikoff, K., Dimitrov, D.S., 2003. The SARS-CoV S glycoprotein: expression and functional characterization. Biochem. Biophys. Res. Commun. 312, 1159–1164.

Yi, C.E., Ba, L., Zhang, L., Ho, D.D., Chen, Z., 2005. Single amino acid substitutions in the severe acute respiratory syndrome coronavirus spike glycoprotein determine viral entry and immunogenicity of a major neutralizing domain. J. Virol. 79, 11638–11646.

Yuan, K., Yi, L., Chen, J., Qu, X., Qing, T., Rao, X., Jiang, P., Hu, J., Xiong, Z., Nie, Y., Shi, X., Wang, W., Ling, C., Yin, X., Fan, K., Lai, L., Ding, M., Deng, H., 2004. Suppression of SARS-CoV entry by peptides corresponding to heptad regions on spike glycoprotein. Biochem. Biophys. Res. Commun. 319, 746–752.

Zheng, B.J., Guan, Y., Hez, M.L., Sun, H., Du, L., Zheng, Y., Wong, K.L., Chen, H., Chen, Y., Lu, L., Tanner, J.A., Watt, R.M., Niccolai, N., Bernini, A., Spiga, O., Woo, P.C., Kung, H.F., Yuen, K.Y., Huang, J.D., 2005. Synthetic peptides outside the spike protein heptad repeat regions as potent inhibitors of SARS-associated coronavirus. Antivir. Ther. 10, 393–403.